

Electron transport and impact ionization in Si

Nobuyuki Sano, Takahiro Aoki, Masaaki Tomizawa, and Akira Yoshii

NTT LSI Laboratories, Nippon Telegraph and Telephone Corporation, 3-1 Morinosato-wakamiya, Atsugi-shi, Kanagawa-ken 243-01, Japan

(Received 6 November 1989; revised manuscript received 5 March 1990)

We examine hot-electron transport with emphasis on the impact-ionization phenomena in crystalline Si using the Monte Carlo method. Contrary to the usual treatment of impact ionization exploiting the Keldysh formula ([Sov. Phys.—JETP 10, 509 (1960)] [Zh. Eksp. Teor. Fiz. 37, 713 (1959)]), a new impact-ionization model which takes account of the wave-vector dependence of the ionization threshold energies associated with a realistic band structure is introduced. The calculation results of impact-ionization properties such as ionization coefficient and quantum yield show excellent agreement with experimental data. The orientational independence of the ionization coefficient and the softness of the ionization threshold in bulk Si are also explained by our ionization model. The present simulations ensure that the approach employed here is a good candidate for correctly describing the impact-ionization mechanism.

I. INTRODUCTION

The study of high-field carrier transport in crystalline Si has been the subject of numerous investigations because of its practical significance in advanced devices such as quarter-micrometer Si metal-oxide-semiconductor field-effect transistors (MOSFET's). It is well known, in particular, that impact ionization plays a major role in such hot-carrier transport.¹ Despite its importance, the understanding of this mechanism is still limited to phenomenological theories in which a few physically ambiguous fitting parameters are usually included.^{1,2}

Among these phenomenological theories, the most widely used are the ones by Shockley,³ Wolff,⁴ and Baraff.⁵ Shockley³ held that impact ionization can be mainly attributed to electrons which completely escape the phonon scatterings and gain sufficient energy to induce impact ionization ("lucky" electron model). This model implicitly implies that the electron energy distribution is *spike-like*. On the other hand, Wolff⁴ argued that the electrons are heated entirely by an external field and by many collisions, and it is these electrons at the high-energy tail of the energy distribution that give rise to impact ionization. Therefore, the electron energy distribution is *assumed* to be *broad*, which contradicts the "lucky" electron model. Wolff's theory explains well the field dependence of the ionization coefficient for high fields, whereas Shockley's theory is a good explanation for low fields.

It is however, extremely difficult to determine the shape of the electron-energy distribution in a way that is consistent with the solution of the Boltzmann equation. Later, both results were obtained as a limiting case of Baraff's theory.⁵ His theory, unfortunately, contains physically ambiguous parameters for best fitting the experimental curve of ionization coefficients and, as a consequence, the physics involved in the ionization processes is still not clear.

An alternative method for tackling impact-ionization

problems is provided by the Monte Carlo method.⁶ The method, in principle, gives first-principles explanation of various transport phenomena, if the band structure and the appropriate scattering mechanisms are exactly embedded. It is, however, quite difficult to incorporate all information in the calculations and some crude approximations are usually employed. A first step toward *completeness* was taken by Hess and co-workers⁷⁻⁹ and by Fischetti and Laux.¹⁰ They implemented the conventional Monte Carlo method by including details of the band structure and the density of states of semiconductor crystals. Unfortunately, the impact-ionization mechanism was treated by the ordinary Keldysh formula,¹¹ which includes two fitting parameters and ignores the anisotropy implied by the realistic band structure.

Recently, we examined the impact-ionization processes and found that the threshold energies specified by the wave vectors of the initiating electrons are of the most importance for determining the ionization probability,^{12,13} namely, the ionization threshold is basically hard even in Si in the sense that electrons rapidly impact-ionize after they exceed the threshold energies. This paper provides a full account of our ionization model and the corresponding results that have already been briefly reported.^{12,13}

We performed the Monte Carlo simulations with a new functional form of the impact-ionization rate, in which wave-vector-dependent ionization thresholds are exploited. It is shown that the excellent agreement obtained between our Monte Carlo calculations and the experimental transport properties for Si *uniquely* leads to the hard threshold in impact ionization and thus substantiates the scenario that the softness of the ionization threshold in Si comes in through the strong wave-vector dependence of the threshold energies. We also provide the results of Monte Carlo simulations, exploiting the ordinary Keldysh formula, expanding on the different interpretations of the impact-ionization mechanism based on our ionization model and on the Keldysh description. It is shown

that our model, although it does not make much difference to the calculation of average energy, or drift velocity, or the ionization coefficient, does make a large difference to the calculation of the quantum yield and thus to the physical mechanism of the impact ionization.

This paper is organized as follows. In Sec. II we describe the impact-ionization model proposed in our earlier papers. Particular attention is paid to the ionization threshold, as the wave-vector dependence of the threshold energies associated with the initiating electrons plays a key role in controlling the ionization rate. In Sec. III the Monte Carlo method employed in the present study is explained with some implementations done for this work. The simulations are presented and discussed in Sec. IV, with emphasis on the physical insights of the impact ionization that can be drawn from our considerations, and which turn out to be quite different from those of the ordinary Keldysh description. Finally, the conclusions are given in Sec. V.

II. IMPACT-IONIZATION MODEL

One of the most important properties in analyzing the impact-ionization mechanism is the ionization rate. It strongly depends on the matrix element through the Coulomb interaction, the degeneracy probabilities of occupancy and vacancy of carriers, and the threshold energy determined from both the energy and momentum conservations.² Exploiting Fermi's Golden rule, the ionization rate $W(\mathbf{k}_1)$ is calculated by

$$W(\mathbf{k}_1) = \frac{2\pi}{\hbar} \frac{1}{(2\pi)^9} \int |M|^2 \delta(E_1 + E_2 - E_3 - E_4) \times f_2(1-f_3)(1-f_4) d^3k_2 d^3k_3 d^3k_4, \quad (1)$$

where \hbar is Planck's constant divided by 2π , M is the matrix element of the Coulomb interaction, and $\delta(x)$ is the δ function for energy conservation. E_i , k_i , and f_i are the energy, wave vector, and distribution function of the i th carrier, respectively. Here $i=1$ corresponds to the initiating electron in the conduction band, $i=2$ the electron in the valence band to be excited, $i=3$ the relaxed initiating electron after ionization, and $i=4$ the relaxed excited electron from the valence band.

Due to the complexity of the band structure at high energies, the microscopic calculation of the ionization rate expressed in Eq. (1) is quite difficult to carry out. To simplify the task, one usually works out the calculation using some approximations. Keldysh assumed that the matrix element is constant and the degeneracy is ignored.¹¹ In fact, these assumptions are not as damaging as they may appear: the most significant factor in the ionization-rate calculation is the threshold energy determined from the energy and momentum conservations.^{12,13} With such assumptions, the ionization rate is defined by¹³

$$w(\mathbf{k}) = C_{ii} \left[\frac{E(\mathbf{k}) - E_{\text{thr}}(\mathbf{k})}{E_{\text{thr}}(\mathbf{k})} \right]^2, \quad (2)$$

where $E(\mathbf{k})$ is the energy of the initiating electron with

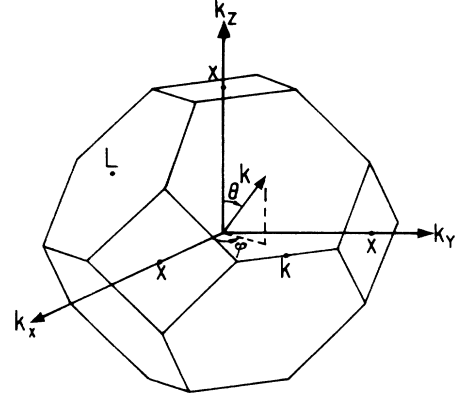


FIG. 1. Coordinate system in wave-vector space employed throughout this work.

wave vector \mathbf{k} and $E_{\text{thr}}(\mathbf{k})$ is the corresponding threshold energy. C_{ii} is a wave-vector-independent constant.

It is noticed that this is a direct generalization of the ordinary Keldysh formula, i.e., averaged over all directions in wave-vector space, Eq. (2) becomes equivalent to the ordinary Keldysh formula, replacing the wave-vector-dependent threshold energy $E_{\text{thr}}(\mathbf{k})$ by a proper wave-vector-independent constant E_{thr} , which is treated as an additional fitting parameter in the Keldysh description. The constant C_{ii} then corresponds to $P/w_{\text{ph}}(E_{\text{thr}})$ in the Keldysh formula,⁷⁻¹⁰ where P is a dimensionless constant and $w_{\text{ph}}(E_{\text{thr}})$ is the phonon scattering rate at the wave-vector-independent threshold energy E_{thr} . We should, however, stress here that, contrary to the Keldysh formula, $w(\mathbf{k})$ in Eq. (2) is a function of the wave vector of the initiating electron and thus is strongly anisotropic. If the band structure is assumed to be isotropic, Eq. (2) becomes independent of the direction of the wave vector and reduces to the ordinary Keldysh formula. It is also appropriate to note that C_{ii} takes into account both hard and soft thresholds, depending on the

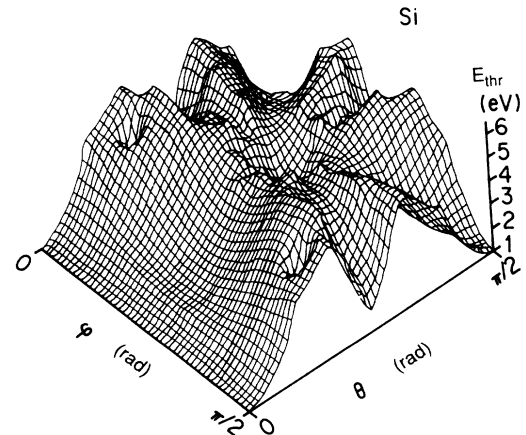


FIG. 2. Ionization threshold energy in Si for various directions of the wave vector of the electron-inducing impact ionization. The polar and azimuthal angles are denoted by θ and φ , respectively. The threshold energies are calculated from a realistic band structure.

magnitude of C_{ii} : the greater the constant C_{ii} , the harder the ionization threshold. Equation (2) is incorporated into the Monte Carlo scheme as a scattering mechanism like the electron-phonon scattering.

The wave-vector-dependent threshold energy $E_{\text{thr}}(\mathbf{k})$, which is a major factor employed in the present work, is calculated from a realistic band structure for crystalline Si by employing the graphical method developed by Anderson and Crowell.¹⁴ Following the argument of Anderson and Crowell, the threshold energy is determined by the direction of the wave vector of the electron giving rise to the impact ionization. In other words, if an exact band structure is known, the threshold energy can be uniquely specified by the polar and azimuthal angles (θ and φ) in wave-vector space.¹² Figure 1 shows the coordinate system in wave-vector space employed here. The band structure for Si is calculated by the empirical pseudopotential method which provides a reliable description of the excitation spectrum of semiconductors.¹⁵ We show the threshold energy thus obtained for various directions of the wave vector of the initiating electron in Fig. 2. Notice that the threshold energy is strongly anisotropic and varies from 1.1 to 6 eV.

III. MONTE CARLO METHOD

The Monte Carlo method employed here is basically similar to the one described by Canali *et al.*¹⁶ Since excellent reviews of the Monte Carlo technique are already available in the literature,^{6,17} we will confine our description here to only those points pertinent to the present study.

The L valleys, in addition to the X valleys, are considered in the program so that the nonequivalent intervalley scattering is included. This is essential because the electric fields experienced by the electrons in the present study are very large (> 100 kV/cm) and the value of the minimum threshold energy (≈ 1.1 eV) is close to the energy separation (≈ 1 eV) (Ref. 15) between the bottoms of X and L valleys. It is highly likely, therefore, for the electrons to exist in the L valleys at high fields, in which the ionization-threshold energies are rather different from those in the X valleys. Also, the locations of each valley in wave-vector space are explicitly incorporated because the X valleys are very anisotropic, with respect to the symmetry lines. As a consequence, the orientational dependence of physical properties such as drift velocity, average energy, ionization coefficient, etc., can be properly analyzed.

The phonon scatterings included in the Monte Carlo program are acoustic intravalley scattering, f and g intervalley scatterings, and nonequivalent intervalley scattering. The material parameters of Si and the coupling constants of intravalley and equivalent intervalley scatterings are taken from the paper by Canali *et al.*¹⁶ These are fixed and kept constant during the present calculations because they are already best fitted from the experimental velocity-field characteristics at low fields (< 50 kV/cm) (Ref. 16) and do not affect the physical properties at the higher fields we are concerned with here. Little is known about the values of the coupling constant D_{XL} of the non-

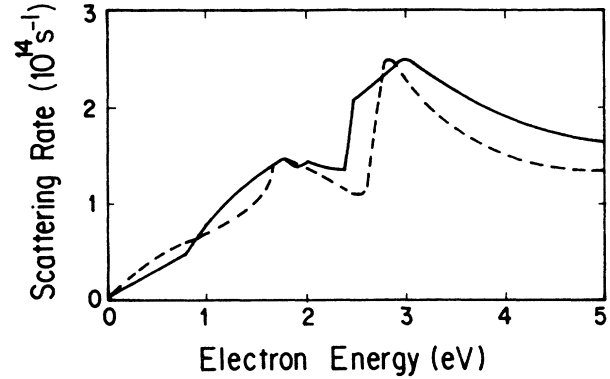


FIG. 3. Total electron-phonon scattering rate for Si at room temperature ($T=300$ K) indicated by the solid line. The broken line is the total electron-phonon scattering rate calculated from the realistic band structure and the density of states of Si (Ref. 10).

equivalent intervalley scattering for four phonons and thus these are assumed to be the same for each phonon, as assumed by Tang and Hess.⁸ The total electron-phonon scattering rates are modified at high energies (> 1.8 eV) such that the high-energy behavior is consistent with the realistic scattering rate given in Ref. 10, which was calculated from the realistic band structure and the density of states. In Fig. 3, the total electron-phonon scattering rate employed here (solid line) is shown as a function of electron energy, with the total electron-phonon scattering rate given in Ref. 10 (broken line).

The impact-ionization process is treated as an additional scattering mechanism. However, we use a different evaluation of the impact-ionization processes instead of the ordinary Keldysh formula, i.e., the wave-vector dependence of the threshold energies, as expressed in Eq. (2), are explicitly incorporated in the ionization scattering rate. Since the trajectory of the simulated electrons is followed in wave-vector space, the ionization scattering rate associated with the wave vector of the initiating electron can be evaluated at each scattering event from Eq. (2).

We wish to stress here that the only fitting parameters included in our model are the coupling constant D_{XL} of

TABLE I. Material parameters in Si. m_0 is the free-electron mass.

Lattice constant	5.431	Å
Density	2.329	g/cm ³
Sound velocity	9.04×10^5	cm/s
Acoustic deformation potential	9	eV
C_{ii} in impact ionization (Eq. 2)	1×10^{15}	s ⁻¹
Nonparabolicity of X valley	0.5	eV ⁻¹
Effective masses (X valley)		
Transverse	0.19	m_0
Longitudinal	0.916	m_0
Effective masses (L valley)		
Transverse	0.12	m_0
Longitudinal	1.59	m_0

TABLE II. Parameters for phonon scatterings in Si.

Phonon energy (meV)	Coupling constant (10^8 eV/cm)	Scattering type
(X-X intervalley scattering)		
18.1	0.15	<i>f</i>
43.1	3.4	<i>f</i>
54.3	4	<i>f</i>
12.1	0.5	<i>g</i>
18.1	0.8	<i>g</i>
60.3	3	<i>g</i>
(X-L intervalley scattering)		
57.9	4	
54.6	4	
41.4	4	
17.0	4	

the X-L intervalley scattering and the constant C_{ii} in Eq. (2). These are *uniquely* determined by best fitting the experimental data of both the ionization coefficient^{18–20} and the quantum yield.²¹ An excellent fit is obtained if the coupling constant is given by $D_{XL} = 4 \times 10^8$ eV/cm, which is close to the value used by Tang and Hess,⁸ and if the constant C_{ii} is given by 1×10^{15} s⁻¹, which corresponds to a large P (hard threshold) in the ordinary Keldysh formula.⁷ Further information pertaining to the value of C_{ii} used here and the corresponding hard ionization threshold for Si will be said below. All material and transport parameters employed throughout the present study are listed in Tables I and II.

IV. RESULTS AND DISCUSSION

With the set of parameters found from the best-fitting procedure proposed above, we performed the Monte Carlo simulations for steady-state transport in single-crystalline Si.

A. High-field electronic transport

The average electron energy thus obtained is shown in Fig. 4 as a function of the electric field directed along the $\langle 111 \rangle$ and $\langle 100 \rangle$ crystallographic directions. The calculations have been done for the temperatures $T=77$ and 300 K. The simulations by Canali *et al.*¹⁶ are also shown with solid and broken lines for the $\langle 111 \rangle$ and $\langle 100 \rangle$ field directions, respectively. Figure 5 shows the drift velocity as a function of the electric field at $T=77$ and 300 K for the $\langle 111 \rangle$ and $\langle 100 \rangle$ field directions, with the experimental data taken from Ref. 16. The low-field (< 50 kV/cm) data of average energy and drift velocity agree very well with the simulation and the experimental data by Canali *et al.*¹⁶ In addition, it is noted that our results also agree well with the simulations by Fischetti and Laux,¹⁰ which take into account the details of the realistic band structure of crystalline Si. This implies that the values for the coupling constants of the intravalley and the equivalent intervalley scatterings found previously by Canali *et al.*¹⁶ properly account for the transport properties even though the higher bands are located close to the

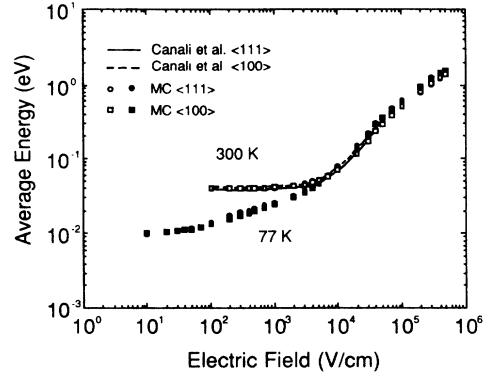


FIG. 4. Average electron energy at $T=77$ (solid) and 300 K (open) as a function of the electric field directed along the $\langle 111 \rangle$ (solid and open circles) and $\langle 100 \rangle$ (solid and open squares) crystallographic directions. Simulation results taken from Ref. 16 are shown with the solid and broken lines for the $\langle 111 \rangle$ and $\langle 100 \rangle$ field directions, respectively.

first conduction-band minimum at the symmetry point X , i.e., the complication of the band due to higher bands at point X is *absorbed* by the proper choice of the values of the coupling constants. Furthermore, the average energy or drift velocity seems to be rather insensitive to the details of the impact-ionization model incorporated in Monte Carlo simulations.

The first maximum drift velocity of about 1×10^7 cm/s is reached at about 50 kV/cm (marked with an arrow in the figure) for $T=300$ K, which is consistent with the results of previous Monte Carlo simulations.^{8,10} In our case, however, the drift velocity does not saturate at fields greater than 50 kV/cm at 300 K, but rather a slight negative differential mobility is seen around 100 kV/cm. This characteristic is also visible when the temperature is lowered ($T=77$ K) and corresponds to the onset of the X-L nonequivalent intervalley scattering taking place at such high fields. Since no experimental data in the range

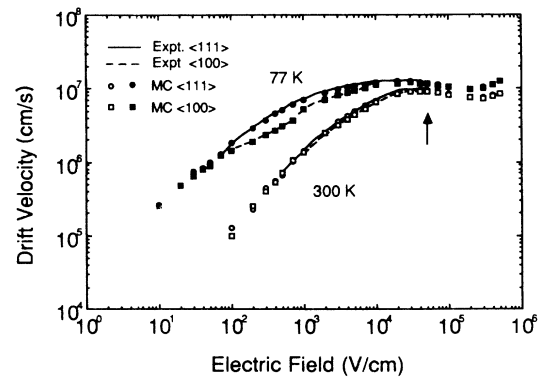


FIG. 5. Simulated electron drift velocity as a function of the electric field along the $\langle 111 \rangle$ (solid and open circles) and $\langle 100 \rangle$ (solid and open squares) crystallographic directions at temperatures $T=77$ (solid) and 300 K (open). The experimental results taken from Ref. 16 are shown with the solid and broken lines for the $\langle 111 \rangle$ and $\langle 100 \rangle$ field directions, respectively.

of high fields (> 100 kV/cm) are available for *bulk* systems, we are unable to draw any conclusions about the negative differential mobility here. Detailed experimental work at such high fields is highly desirable.

B. Impact-ionization mechanism

Figure 6 shows the ionization coefficient obtained from our simulations for the electric field along the $\langle 111 \rangle$ and $\langle 100 \rangle$ crystallographic directions at $T=300$ K. Experimental data taken from Refs. 18–20 are shown for comparison. The agreement between our results and the experimental data is good. The simulations for the $\langle 111 \rangle$ and $\langle 100 \rangle$ field directions are so close that we do not observe any orientational dependence of the ionization coefficients. This is very interesting because the ionization scattering rate employed here is strongly anisotropic, on the contrary to the ordinary Keldysh formula.

The solution to this puzzle is that the electrons with high energies are mainly scattered via both the equivalent and the nonequivalent intervalley scatterings, by which the electrons tend to fill, almost uniformly, the entire Brillouin zone (BZ). The population of electrons in the BZ is, therefore, almost independent of the field direction at such high fields. On the other hand, impact ionization occurs at the points in wave-vector space where the ionization threshold energy is relatively small: electrons farther away from the symmetry lines such as the ΓX or ΓL line hardly impact-ionize at all because of the large threshold energies, as seen in Fig. 2. Hence, the orientational dependence of the ionization coefficients, with respect to the electric-field direction is hidden by the almost uniform population of electrons in the BZ. The above argument is well described in Fig. 7, in which the locations of the electrons in wave-vector space giving rise to the impact ionization are shown for the electric field of $F=500$ kV/cm directed along the $\langle 111 \rangle$ and $\langle 100 \rangle$ crystallographic directions. No significant difference between the two different field directions is seen, as we would expect.

In fact, the similar argument holds true for the case that the isotropic threshold energy, implied by the ordi-

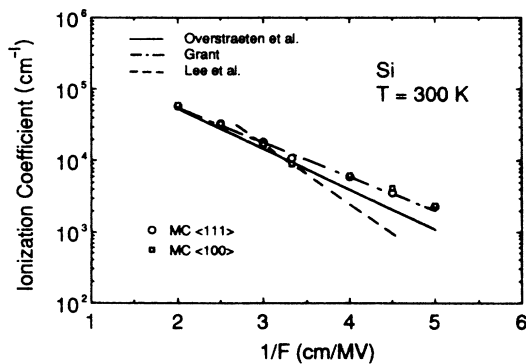


FIG. 6. Simulated ionization coefficient for the electric field along the $\langle 111 \rangle$ (circle) and $\langle 100 \rangle$ (square) crystallographic directions at $T=300$ K. Experimental data are taken from Refs. 18–20 and are indicated by the lines.

nary Keldysh formula, is employed in the Monte Carlo calculations. It is, therefore, quite reasonable that one has obtained the orientation-independent ionization coefficient in the past Monte Carlo simulations.^{8,10} However, the physical processes of the impact ionization behind the two models are rather different. In order to emphasize this point, we have done the simulations by exploiting the ordinary Keldysh formula.

As we mentioned in Sec. II, the Keldysh formula contains two fitting parameters (P and E_{thr}) and these are usually determined by fitting the experimental ionization coefficient. It is not, however, possible to *uniquely* fix the parameters, and at *least* two sets of parameters corresponding to soft and hard ionization thresholds have been found: $P=0.01$ and $E_{\text{thr}}=1.1$ eV (soft threshold) and $P=100$ and $E_{\text{thr}}=2.0$ eV (hard threshold). These turn out to be similar to those found by Tang and Hess.⁸ As we will show in the calculation of quantum yield below, the soft threshold parameters give a better fit to the experimental findings, consistently with the previous finding by Tang and Hess.⁸ With the soft threshold condition, the locations of the electrons giving rise to the impact ionization obtained by the Keldysh formula are shown in Fig. 8 for $F=500$ kV/cm along the $\langle 111 \rangle$ and

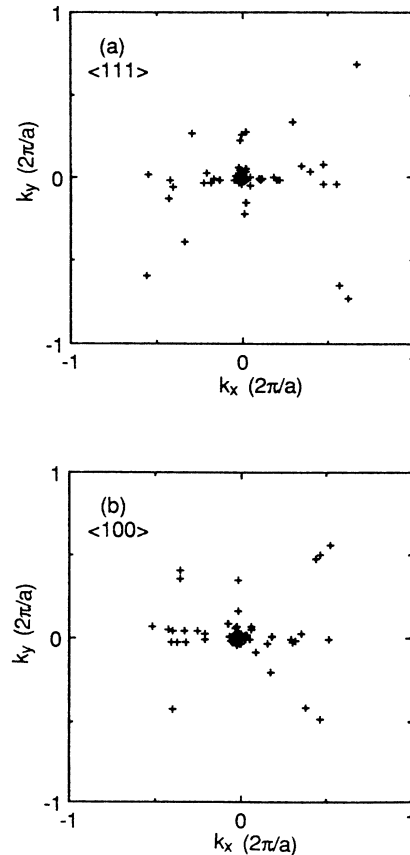


FIG. 7. Population of 60 electrons, obtained from the present model, in wave-vector space giving rise to impact ionization at $T=300$ K for the electric field $F=500$ kV/cm along the (a) $\langle 111 \rangle$ and (b) $\langle 100 \rangle$ crystallographic directions. Projection onto the $k_x - k_y$ plane is shown.

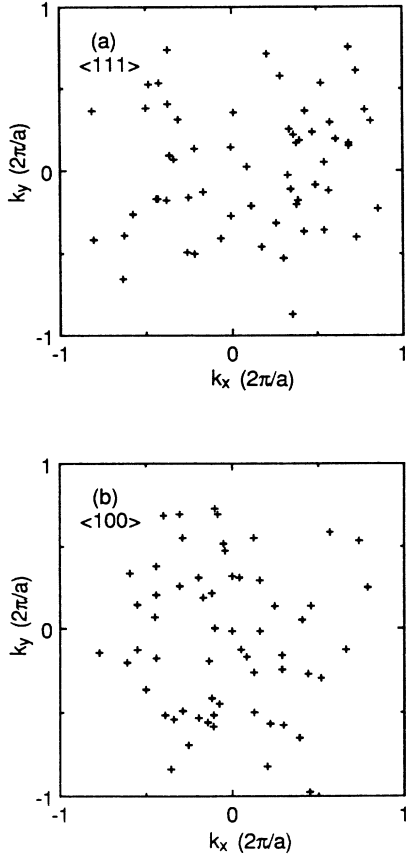


FIG. 8. Population of 60 electrons, obtained from the Keldysh formula with the soft threshold, in wave-vector space giving rise to impact ionization at $T=300$ K for the electric field $F=500$ kV/cm along the (a) $\langle 111 \rangle$ and (b) $\langle 100 \rangle$ crystallographic directions. The projection onto the $k_x - k_y$ plane is shown.

$\langle 100 \rangle$ crystallographic directions. The electrons inducing the impact ionization are almost uniformly distributed in the BZ, no matter which direction the electric field follows, and thus anisotropy of the ionization coefficient would not be expected. However, the populations of the electrons obtained from the Keldysh description are very different from those by our model (see Figs. 7 and 8), namely, the electrons away from the symmetry lines also impact-ionize in the Keldysh description. Because of the lack of direct experimental evidence, it is difficult to do justice to the description of impact ionization that is close to the physical reality. However, the superiority of our model is clearly seen in the calculation of quantum yield.

The quantum yield is calculated by the Monte Carlo method in the following way. Many electrons with some specific energy are injected into Si and the trajectories of these electrons are followed in wave-vector space until the energies of the electrons become well below the minimum of the threshold energies (≈ 1.1 eV). The quantum yield is then given by simply taking the ratio of the number of impact-ionization events to the total injected electrons.

The simulation results of quantum yield at $T=300$ K are shown in Fig. 9 with the experimental data.²¹ The simulations have been performed employing our model and the ordinary Keldysh model with both the soft and hard threshold conditions. The soft threshold parameters indeed give a better fit to the experimental quantum yield compared to the hard threshold parameters. However, because of the uniformity of the threshold energy, the Keldysh description with the soft threshold gives a monotonically increasing quantum yield. On the other hand, our model produces a much better fit to the experimental data, in spite of one less fitting parameter included in our description. We may, therefore, say that our model more accurately describes the impact-ionization processes than the ordinary Keldysh description.

Furthermore, notice that the quantum yield is a direct measure of the effective ionization threshold²¹ and thus of the softness of the ionization threshold. The effective ionization threshold energy (≈ 1.7 eV), despite the hard ionization threshold (large C_{ii}) employed in our model, is clearly greater than the minimum threshold energy (≈ 1.1 eV) for Si, and this is consistent with the experimental findings.²¹ In our model, the *uniquely* determined parameter C_{ii} implies a hard ionization threshold, contrary to the previous Monte Carlo simulations^{8,10} in which a soft threshold, as expected from the plot of Fig. 9, has usually been *assumed* in Si for a better description of transport properties at extremely high fields. In fact, the detailed calculation of the ionization scattering rate shows a rather slow rise as a function of electron energy.²² This seeming contradiction can be resolved again by the wave-vector dependence of the threshold energies.

In the case of hard threshold, electrons exceeding the threshold energies rapidly impact-ionize, whereas electrons do not immediately impact-ionize above the threshold energies in the case of a soft threshold. However, the threshold energy included in Eq. (2) strongly depends on the direction of the wave vector of the initiating electron. The variation of the threshold energies, with respect to the direction of the wave vector is quite large for Si, as

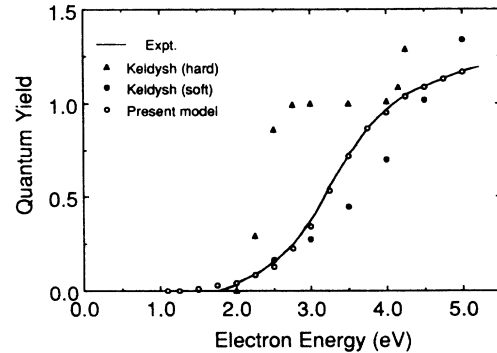


FIG. 9. Quantum yield (open circle) calculated from the present model at $T=300$ K. Simulations obtained from the ordinary Keldysh formula with the two sets of parameters corresponding to soft (solid circle) and hard (solid triangle) ionization thresholds are also shown. Experimental data (solid line) are taken from Ref. 21.

shown in Fig. 2. On the other hand, the electrons gradually populate the entire BZ as the electron energy increases. The number of electrons capable of impact ionization, therefore, increases very slowly for Si as the electric field becomes greater. As a consequence, the rise of quantum yield near the minimum threshold energy (≈ 1.1 eV) becomes slow and, correspondingly, the effective ionization threshold becomes much greater than the minimum threshold energy for Si.

It is also instructive to note that the constant C_{ii} in Eq. (2) is of the order $e^4 m^* / \hbar^3 \approx 10^{16} \text{ s}^{-1}$ for direct-band gap semiconductors like GaAs,¹¹ corresponding to a large P (hard threshold) in the ordinary Keldysh formula. Here e is the electronic charge and m^* is the effective mass of an electron in a semiconductor. Since Si has an indirect gap in which many transitions occur with the help of phonons, an additional softness is introduced in the matrix element, and thus in the constant C_{ii} . Therefore, the value $C_{ii} = 1 \times 10^{15} \text{ s}^{-1}$ found here is quite reasonable. In addition, the fact that the value $Pw_{\text{ph}}(E_{\text{thr}}) = 2.5 \times 10^{15} \text{ s}^{-1}$ for GaAs used by Fischetti and Laux¹⁰ is similar to that of C_{ii} found here, strongly substantiates our earlier proposition: that the ionization threshold is basically hard even in Si, whereas the strong wave-vector dependence of the threshold energy causes the softness of the ionization threshold.

V. CONCLUSIONS

We have performed Monte Carlo simulations on impact ionization at extremely high fields by exploiting a new impact-ionization model. The introduction of the wave-vector-dependent threshold energy is a key factor in the present work that plays a major role in controlling the physical processes of impact ionization. The calculation results based on our model agree very well with the experimental data of impact-ionization properties such as the ionization coefficient and quantum yield. The orientational independence of ionization coefficient and the softness of ionization threshold in bulk Si are explained in terms of the wave-vector dependence of the threshold energies. The present study ensures that the wave-vector-dependent approach we have presented here is a good candidate for correctly describing impact-ionization phenomena.

ACKNOWLEDGMENTS

Special thanks are due to Dr. K. Yokoyama and Dr. A. Ishida for their constant support and encouragement during this work.

-
- ¹F. Capasso, in *Semiconductors and Semimetals*, edited by R. K. Willardson and A. C. Beer (Academic, New York, 1985), Vol. 22, p. 1.
- ²D. J. Robbins, *Phys. Status Solidi B* **97**, 387 (1980); **98**, 11 (1980).
- ³W. Shockley, *Solid-State Electron.* **2**, 35 (1961).
- ⁴P. A. Wolff, *Phys. Rev.* **95**, 1415 (1954).
- ⁵G. A. Baraff, *Phys. Rev.* **128**, 2507 (1962).
- ⁶C. Jacoboni and L. Reggiani, *Rev. Mod. Phys.* **55**, 645 (1983).
- ⁷H. Shichijo and K. Hess, *Phys. Rev. B* **23**, 4197 (1981).
- ⁸J. Y. Tang and K. Hess, *J. Appl. Phys.* **54**, 5139 (1983).
- ⁹K. Kim, K. Kahen, J. P. Leburton, and K. Hess, *J. Appl. Phys.* **59**, 2595 (1986).
- ¹⁰M. V. Fischetti and S. E. Laux, *Phys. Rev. B* **38**, 9721 (1988).
- ¹¹L. V. Keldysh, *Zh. Eksp. Teor. Fiz.* **37**, 713 (1959) [*Sov. Phys.—JETP*, **10**, 509 (1960)].
- ¹²N. Sano, T. Aoki, and A. Yoshii, *Appl. Phys. Lett.* **55**, 1418 (1989).
- ¹³N. Sano, M. Tomizawa, and A. Yoshii, *Appl. Phys. Lett.* **56**, 653 (1990).
- ¹⁴C. L. Anderson and C. R. Crowell, *Phys. Rev. B* **5**, 2267 (1972).
- ¹⁵M. L. Cohen and T. K. Bergstresser, *Phys. Rev.* **141**, 789 (1966).
- ¹⁶C. Canali, C. Jacoboni, F. Nava, G. Ottaviani, and A. Alberigi-Quaranta, *Phys. Rev. B* **12**, 2265 (1975).
- ¹⁷P. J. Price, in *Semiconductors and Semimetals*, edited by R. K. Willardson and A. C. Beer (Academic, New York, 1979), Vol. 14, p. 249.
- ¹⁸C. A. Lee, R. A. Logan, R. L. Batdorf, J. J. Kleimack, and W. Wiegmann, *Phys. Rev.* **134** A761 (1964).
- ¹⁹W. N. Grant, *Solid-State Electron.* **16**, 1189 (1973).
- ²⁰R. van Overstraeten and H. DeMan, *Solid-State Electron.* **13**, 583 (1970).
- ²¹C. Chang, C. Hu, and R. W. Brodersen, *J. Appl. Phys.* **57**, 302 (1985).
- ²²E. O. Kane, *Phys. Rev.* **159**, 624 (1967).